Characterization of Phenol-Formaldehyde Resins Modified with Crude Bio-oil Prepared from *Ziziphus mauritiana* Endocarps

Shakir Ahmad Shahid,[a] Muhammad Ali,[a] and Zafar Iqbal Zafar [b,*]

This study was conducted to evaluate the effects of bio-oil incorporation on properties of bio-oil-phenol formaldehyde (BPF) resol resins along with the optimization of petro-phenol substitution level. Crude bio-oil prepared from endocarp shells of *Ziziphus mauritiana* by direct solvolytic liquefaction (ethanol-water 1:1 wt./wt. at 300 °C) was used to partially substitute the petro-phenol (30% to 75% wt./wt.) in the resin synthesis. The modified resins were subjected to measurement of various properties, including molecular weight, pH, viscosity, density, gel/cure time, non-volatile solid content, and limiting oxygen index. Bonding performance of the BPF resins was evaluated by measuring the mechanical and hygroscopic properties of the particle boards developed using such resins. With the incorporation of bio-oil, the viscosity and molecular weight of the BPF resins increased, while the values of pH, density, non-volatile solid content, and limiting oxygen index decreased. The gel, cure, and bonding tests revealed that with the addition of more than 45% bio-oil, the gel/cure times of the BPF resins increased, while the bonding performance decreased. Petro-phenol could therefore be substituted by crude bio-oil up to 45% wt./wt. safely.

Keywords: Crude bio-oil; Bio-wastes; Ziziphus mauritiana; Bio-oil phenol formaldehyde resins; Gel permeation chromatography; Molecular weight; Particle boards; Mechanical and hygroscopic strength

Contact information: a: Department of Chemistry, University of Sargodha, Sargodha-40100, Pakistan;
b: Institute of Chemical Sciences, Bahauddin Zakariya University, Multan-60800, Pakistan;
** Corresponding author: drzafarbzu@hotmail.com*

INTRODUCTION

Phenol-formaldehyde (PF) resin is the most widely used thermosetting adhesive employed in manufacturing for wood-based composite materials (Frihart 2005). PF resin possesses many advantages, such as readily available raw materials, simple production processes, and good mechanical and hygroscopic strength. The literature indicates that PF resin is a major adhesive used in exterior grade wood-based panels (Knop and Pilato 1985; Sellers 1985). However, the marked disadvantages of the PF resin are relatively longer cure and press times, dark colored bond line, environmental issues of toxicity, and non-biodegradation.

Phenol, which is the basic raw material used in development of PF resin, is derived from petroleum-based resources. However, with ever increasing demand for petrochemicals along with continuously declining reserves of petroleum, the sustainable supply of phenol has become a serious issue. Hence, over the past few decades, environmental issues and sustainability have become the main drivers of research to produce eco-friendly materials developed from renewable resources. In this respect,

considerable research has been conducted to replace petro-materials with different kinds of bio-materials extracted from renewable bio-resources (Zhang *et al.* 2006, 2013).

Amongst various possible alternative bio-materials, liquefied lignocellulosic biomass holds an immense potential to replace petro-phenol in various applications. Lignocellulosic biomass primarily consists of the natural polymers hemicelluloses (15 to 35 wt.%), cellulose (35 to 45 wt.%), and lignin (10 to 35 wt.%) (Gani and Naruse 2007; Sanchez 2009). Lignin, which is the second most abundant polymer found in nature, is a polyphenolic compound containing three main phenyl-propanols, termed monolignols, *i.e.*, guaiacyl-propanol (G), syringyl-propanol (S), and p-hydroxyl-phenyl-propanol (H) (Weng *et al*. 2008). Thus after depolymerizing the lignocellulosic fractions, the treated biomass can serve as a potential source of bio-phenols.

Drupe endocarp biomass, which is a major forest and agricultural bio-waste, is produced all over the world. On average, the drupe endocarp comprises 42% lignin, 30% cellulose, and 1.5% ash by weight, and is considered as one of the highest lignin containing biomass feedstocks (Dardick *et al.* 2010; Mendu *et al*. 2011). The total estimated yield of endocarp for the year 2000 was 2.4×10^7 tons, with a high production density in South Asia, including Pakistan (Mendu *et al.* 2012). *Ziziphus mauritiana*, which is commonly known as "bair" or "beer" in local languages, is an abundantly found fruit plant in Pakistan. Generally, after eating the fleshy portion (mesocarp) of the fruit, the endocarp stone is discarded as a waste material. However, this endocarp bio-waste can be utilized for extracting of a variety of useful materials, including bio-phenols.

Various biological, chemical, and thermal routes (Briens *et al.* 2008; Xu *et al.* 2008) have been adopted for extraction of different bio-phenolic products, such as bio-oil, from lignocellulosic biomass. Pyrolysis and liquefaction are the two main thermochemical technologies in practice to produce bio-oils. Generally the liquefaction occurs at 50 to 200 atm and 250 to 450 °C, while the pyrolysis occurs at 1 to 5 atm and 375 to 525 °C. Though the capital cost of liquefaction bio-oil is generally high as compared to the pyrolysis oils (Huber *et al.* 2006), the liquefaction technique is more promising in terms of quality parameters of the produced bio-oil.

In thermochemical production of bio-oil the macromolecular bio-mass is fragmented into a variety of small molecules. The chemical and physical nature of the produced bio-oil depends on reaction parameters of the production technique. Chemically the bio-oils are a mixture of more than 400 different compounds, including alcohols, acids, aldehydes, esters, and ketones (Elliott *et al.* 1991). Generally, the extracted bio-oil contains 5 to 10% organic acids, 5 to 20% aldehydes and hydroxyaldehydes, 0 to 10% ketones and hydroxylketones, 20 to 30% phenolics, and 15 to 30% water (Sukhbaatar *et al.* 2009).

Generally the bio-oils have certain limitations such as low heating value, high moisture content, instability and corrosiveness (Özbay *et al.* 2006). Typically the pyrolysis oils have high moisture content (15 to 30 wt. %), high acidity (pH 2.5), high oxygen content (35 to 40 wt.%), low viscosity (40 to 100 cP @50 °C), and low higher heating value (16 to 19 MJ/kg) as compared to the oils produced by the liquefaction process, and hence need upgradation before being used for any purposes (Huber *et al.* 2006). However, the bio-oil, especially the liquefaction bio-oil can be employed directly as a source of bio-phenols in various applications (Effendi *et al.* 2008; Wang *et al.* 2009b; Tymchyshyn and Xu 2010; Cheng *et al.* 2011).

The substitution of petro-phenol with bio-oil extracted from liquefied bio-mass has been studied extensively (Alma and Basturk 2006; Amen-Chen *et al.* 2002; Cheng *et*

al. 2011), but it is still a challenging issue in many aspects. Two major challenges faced during such substitution are the high molecular weights and low reactivity of the extracted bio-oils. It is reported that there is a shortage of low-molecular weight monophenolic compounds with unoccupied active sites in bio-oils (Lee *et al.* 2000). Various methods of extraction and modification have been used to overcome the problem of relatively low reactivity and high molecular weights of the extracted bio-oils.

Amongst various extraction techniques aimed at enhancing the reactivity of bio-oils, direct solvolytic liquefaction method is one that merits special attention. It is generally believed that direct solvolytic liquefaction is not only an effective, economical, and eco-friendly process, but it also produces low-molecular weight bio-oil with enhanced reactivity. The liquefaction of biomass in sub-/super-critical solvents like water, alcohols, and phenol has proven to be an effective and promising approach (Alma *et al.* 2001; Cheng *et al.* 2010; Cheng *et al.* 2011; Lee and Ohkita 2003; Mun *et al.* 2007) for the production of such bio-oils.

The purpose of the present study is to develop a suitable synthesis of bio-oil-phenol formaldehyde (BPF) adhesive resins by utilizing locally available bio-wastes as a source of crude bio-oil with the broad objective of developing eco-friendly sustainable materials from such waste biomass and renewable resources. The present work is conducted to evaluate the effects of bio-oil incorporation (BOI) on various physical, thermal, and bonding properties of the BPF resins, along with the optimization of BOI levels in the PF resin formulations.

EXPERIMENTAL

Materials

The ACS reagent-grade chemicals (ethanol, methanol, acetone, and ethyl acetate, 2 N Folin-Ciocalteu reagent, Karl Fischer reagent, gallic acid) supplied by Sigma-Aldrich (St Louis, MO, USA) were used as received. Commercial-grade phenol of 99% purity, formaldehyde solution (35 wt.% aqueous solution), and sodium hydroxide (40 wt.% aqueous solution) were also used. In gel permeation chromatography (GPC) analysis, high performance liquid chromatography (HPLC)-grade solvents (methanol, tetrahydrofuran (THF) containing 0.03% 2,6-di-tert-butyl-4-methylphenol stabilizer, and water) were used. The waste endocarp stones of *Ziziphus mauritiana* were collected from a rural location in district Jhang (Pakistan).

Methods

Preparation of powdered endocarp shells of Ziziphus mauritiana

The endocarp stones were first washed thoroughly with fresh water and then dried in hot air at 100 °C. The dried stones were crushed by a jaw crusher to a coarse size of 1 to 3 mm, and then the shell part of the ground mixture was separated from the seed part using a flotation process. The dried shell particles were ground and sieved to *ca*. 20-mesh size. The ground powder was further dried under vacuum at 100 °C for 8 h until a constant weight was achieved and then stored in a desiccator for use in the liquefaction process.

Preparation of crude bio-oil by liquefaction of powdered endocarp biomass

The liquefaction of powdered biomass was carried out according to the procedure reported by Cheng *et al.* (2010) with some suitable modifications. A 1000-mL Parr high-pressure stainless steel autoclave equipped with a stirrer and cooling unit was used. In a typical run, the reactor was charged with 50 g of biomass powder and 500 g of an ethanol-water (1:1 wt./wt.) co-solvent mixture. After displacing the inside air, the reactor was pressurized to 2.0 MPa with nitrogen. The reactor was heated to 300 °C at a steady rate of 10 °C/min and kept at this temperature for 15 min before it was cooled. After venting the gaseous products, the processed biomass was rinsed thoroughly with acetone, and liquid products were separated from the solid residue by filtration. The ethanol and acetone were evaporated from the filtrate solution under vacuum at 40 °C, and the remaining liquid solution was extracted with ethyl acetate using a separatory funnel. The ethyl acetate soluble phase was evaporated under reduced pressure at 57 °C to produce crude bio-oil.

Characterization of the prepared crude bio-oil

The water content of the crude bio-oil was determined by Karl Fischer titration according to ASTM D1744-13. The density of the bio-oil was determined by measuring the mass of a known volume of the bio-oil in a graduated cylinder. The density was calculated as: Mass of bio-oil/Volume of bio-oil. The viscosity of the bio-oil was measured according to ASTM D5018-89 by using Synchro-Lectric Viscometer (Brookfield Engineering Laboratories, Stoughton, Mass.).

The higher heating value (HHV) of the bio-oil was measured according to ASTM D240-09 by oxygen bomb calorimeter (Parr, USA). The carbon residue (wt. %) of the bio-oil was determined according to ASTM D4530-11 by heating the bio-oil sample at 500 °C under inert (nitrogen) atmosphere in a controlled manner. The ash residue (wt. %) of the bio-oil was determined according to ASTM D482-13.

The pH value of the bio-oil was determined using a digital pH meter (CyberScan pH 510, Eutech Instruments; Singapore). The total phenol content of the bio-oil was determined by the Folin-Ciocalteu (FC) method as reported by Gutfinger (1981), with some modifications. The absorbance was measured with use of a Shimadzu UV-1800 Spectrophotometer, Japan. Quantification of the total phenol content was made on the basis of standard curve of gallic acid and results were expressed as milligrams of gallic acid equivalent (mgGAE/g). The total acid number (TAN) of the bio-oil was measured according to ASTM D664-11.

The molecular weight of the extracted bio-oil was determined by employing a Waters Breeze gel permeation chromatograph (Waters, Milford, MA; 1525 binary HPLC pump; RI detector at 30 °C; UV detector at 270 nm; Waters Styragel HR1 column at 40 °C) with THF as the eluent at a flow rate of 1 mL/min and polystyrene as the calibration standard. GC-MS analysis of the bio-oil was conducted on a GCMS-QP2010 Plus spectrometer (Shimadzu, Japan) equipped with RTX-5MS capillary column (5% biphenyl 95% dimethyl polysiloxane, 30 m×0.25 mm×0.25µm), at a temperature program of 40 °C (hold 2 min), 190 °C (12 C/min), 290 °C (8 °C /min, hold 20 min).

Synthesis of conventional PF and bio-oil phenol formaldehyde resins

Resol-type phenol-formaldehyde resins were synthesized according to the procedure reported by Alma *et al.* (2001) with some modifications. A three-necked 100-mL flask equipped with a magnetic stirrer and cooling unit was used. Phenol and

formaldehyde were used at a molar ratio of 1:2, while NaOH as a catalyst was used in an amount corresponding to a 0.1:1 molar ratio of NaOH/phenol. For preparation of conventional PF (CPF) resin, the calculated amounts of phenol, sodium hydroxide solution (50 wt.%), and water (to make up 45% solids) were charged into the reaction flask. Then, 10 mL of ethanol was added to the reaction mixture to keep the mixture homogeneous. The temperature of the reaction medium was gradually raised to 80 °C and maintained at this temperature for 1 h under continuous stirring. Then, the calculated amount of formaldehyde (*ca*. 37 wt.%) was added drop wise. After keeping the reaction medium at 80 °C for 3 h, the reaction was stopped by rapid cooling. The ethanol in the flask was evaporated at 60 °C under reduced pressure to produce a dark-brown viscous resin solution that was stored at room temperature.

The bio-oil phenol formaldehyde (BPF) resins were synthesized by replacing the phenol with an equivalent amount of bio-oil at incorporation levels of 30, 45, 60, and 75 wt.% of phenol, and were coded BPF30, BPF45, BPF60, and BPF75, respectively. The solid form of the resins was obtained by neutralizing the resin solution to pH 6.5 using aminosulfonic acid and then air-dried to amorphous powdered form. The synthesized resins were stored in a desiccator for use in various experimental studies.

Characterization of the synthesized resin samples

The molecular weights of the resins and their distributions were analyzed employing the Waters Breeze gel permeation chromatograph (1525 binary HPLC pump; RI detector at 30 °C; UV detector at 270 nm; Waters Styragel HR1 column at 40 °C), using THF as the eluent at a flow rate of 1 mL/min; polystyrene standards were used for calibration. To improve the resins' solubility in THF, the resins were acetylated by dissolving 0.5 g of resin in 10 mL of a mixture (1:1 v/v) of pyridine and acetic acid, followed by magnetic stirring at room temperature for 24 h. The acetylated resin was precipitated in ice-cooled 1.0 wt.% HCl solution, filtered, rinsed thoroughly with distilled water, and then vacuum dried at room temperature.

The pH value of the resins was determined using a digital pH meter (CyberScan pH 510, Eutech Instruments; Singapore) by inserting the pH meter electrode into the resin solution. The density of the liquid resin was determined by measuring the mass of a known volume of the liquid resin in a graduated cylinder. The density was calculated as: Mass of liquid resin/Volume of liquid resin. The viscosity of the liquid resins sample was measured by a Brookfield CAP 2000+ viscometer (Brookfield Engineering Laboratories; Middleboro, MA) according to ASTM D1084-97 (2005).

The gel time of the resins was measured using a Sunshine gel meter (Sunshine, Philadelphia, PA) with a water bath at 100 °C. All tests were made with 10 g of the resin sample conditioned to room temperature. A test tube containing 6.5 g of the resin was immersed in a water bath maintained at 100 °C. The time count was started immediately, while the resin was mixed continuously with a glass rod. The time was measured in seconds when the resin could not flow down from the glass rod. Five trials were performed for each type of sample to measure the gel time.

The resin sample containing hexamine (15% of dry wt. of resin) as a curing agent was heated isothermally at 120 °C on a temperature-controlled hot plate until the resin solidified into a brittle hard material. The time required for solidification is given as the cure time. Five trials were performed for each type of sample to measure the curing times.

The non-volatile solid content of the resin was determined according to ASTM D4426-01 (2006) by oven drying the resin sample at 125 °C for 2 h. The flame retardation property of the resins was evaluated by measuring the limiting oxygen index (LOI) of the resin sample on a Stanton Redcroft flame meter (Stanton Redcroft, UK) according to ASTM D-2863-77 (revised 1990).

Development of randomly oriented medium-density single-layered particle boards

Sawdust from locally available Shisham wood (*Dalbergia sissoo*) was air-dried to a moisture content of 7 wt. % and then sieved through a 35 mesh (Tyler standard) screen size. The screened particles were mixed with hexamine as a hardener (15 wt. % of the resin) and then transferred to blenders where a calculated amount of adhesive (9 wt. % of the oven dry weight of the particles) was sprayed onto the mixture. Before using the BPF resin as an adhesive, the alkali content was increased to that of the CPF resin to compensate for the deficit of sodium hydroxide. The whole mixture was blended for 8 to 10 min, air-dried to 7 wt. % moisture content, and then formatted into a single-layered consistent loose mat. The loose mat was first cold-pressed and then hot-pressed at specific conditions of pressure, temperature, and time to fabricate board sheets of specific dimensions. The fabricated sheet was conditioned in an oven at 180 °C for 1 h to cure the used resin completely. After trimming the fabricated board sheets, board samples of specified sizes were cut. The particle board samples utilizing different types of resin *viz.*, CPF, BPF30, BPF45, BPF60, and BPF75, were denoted B.CPF, B.BPF30, B.BPF45, B.BPF60, and B.BPF75, respectively.

Testing of bonding performance of the resin samples by measuring the mechanical and hygroscopic properties of the developed particle boards

All the board samples were conditioned at room temperature (25 °C) and a relative humidity (RH) of 65 ± 5% for 12 days before testing. Mechanical properties, including modulus of rupture (MOR) and internal bond strength (IB), were measured according to ASTM-D 1037-99 (1999) using an Instron Universal Testing Machine Model 4204 (Canton, MS) at room temperature (25 °C). The boiled IB value was measured by boiling the board samples in neutral water (pH~7) for 2 h, oven drying for 6 h at 103 °C, and then equilibrating to 7% moisture content. The water absorption (WA %) and thickness swelling (TS %) were measured by submerging the board samples in neutral water at 100 °C for 2 h, drip-drying for 10 min, and then wiping the surface clean of water.

RESULTS AND DISCUSSION

Properties of the Prepared Crude Bio-Oil

The measured values of water content, density, viscosity, carbon residue, ash residue, and higher heating value of the bio-oil are presented in Table 1. The measured value of the water content of the bio-oil was 5.5 wt.%, which is comparable with the results reported earlier in case of liquefaction oils (Huber *et al.* 2006); however, it was much lower than the typical water content of 24.8 wt.% in case of pyrolysis oils (Elliott and Schiefelbein 1989). The water content of bio-oil is an important parameter regarding its storage, viscosity, heating value, and combustion perspectives (Lu *et al.* 2009). The measured value of density of the bio-oil was 1.213 (g/cm^3), which is comparable with the

results reported earlier in case of liquefaction oils; however, it was higher than the typical density value of 0.94 (g/cm^3) for heavy fuel oil (Huber *et al.* 2006). The relatively higher value of bio-oil density may be attributed to the presence of high molecular weight bio-oil molecules indicated by GC-MS and GPC studies, as already cited in literature (Oasmaa and Czernik 1999).

Table 1. Water Content, Density, Viscosity, Carbon Residue, Ash Residue, and Higher Heating Value of the Bio-oil

Physical properties		Thermal properties	
Water content (wt. %)	5.5 (± 0.11)	Carbon residue (wt. %)	15.25 (± 0.085)
Density (g/cm^3)	1.213 (± 0.005)	Ash residue (wt.%)	0.275 (± 0.018)
Viscosity (cP) @25°C	2940 (± 3.89)	Higher heating value (MJ/kg)	39.21 (± 0.392)
*Each value represents an average of three samples (± SEM)			

The measured value of the bio-oil viscosity was 2940 (cP), which is comparable with the results reported earlier in case of liquefaction oils (He *et al.* 2001). However, it is much higher than the typical viscosity range of 40 to 100cP@50 °C for pyrolysis oils, and typical viscosity of 180cP for heavy fuel oil (Huber *et al.* 2006). The high viscosity value may be attributed to high molecular weight bio-oil molecules (Venderbosch and Prins 2010) as indicated by GC-MS and GPC studies, and to low water content of bio-oil. The high viscosity value may also be attributed to the dragging effect of the side chains attached on bio-oil molecules, as shown by GC-MS study. During various syntheses the viscosity of crude bio-oil may be taken as an indirect indication of the bio-oil reactivity as it is generally believed that higher is the depolymerization of the bio-mass more is the expected reactivity of the resulting product. Furthermore the viscosity is a critical parameter during pumping and injecting of bio-oil during its process handlings.

The measured value of carbon residue of the bio-oil was 15.25 wt.%, indicating its thermal instability and coke forming tendency at elevated temperatures. The thermal instability may be attributed to the presence of unsaturated double bonds, oxygenated molecules (He *et al.* 2001b; Yao *et al*. 2008), and side chains attached on bio-oil molecules (Wang *et al.* 2009a). The weight loss during thermal heating may also be attributed to thermal degradation of cellulosic impurities, and removal of water and other volatile molecules present in the crude bio-oil. The double bonds containing molecules such as aldehydes, ketones, and alkenyls determine the thermal instability of the bio-oil (Yao *et al.* 2008). The thermal instability of the oxygenated molecules may be attributed to the presence of lone pair of electrons on oxygen atom which becomes more active for electrophilic reactions at elevated temperatures. However, in case of phenolic hydroxyl group the oxygen lone pair of electrons is resonating over all of the benzene ring, and resultantly less available during thermal reactions. Hence it can be assumed that non-phenolic molecules such as alcohols, ketones, aldehydes, and carboxylic acids are more prone to thermal reactions resulting in char formation, as indicated in literature (Diebold 2000; Oasmaa and Kuoppala 2003). At elevated temperatures a number of reorganization and repolymerization reactions are involved in coke formation, as reported in literature (Khan and Ashraf 2007; Chen *et al.* 2008; Wang *et al.* 2009a; Cheng *et al.* 2011, 2012).

The measured value of ash residue on combustion of the bio-oil was 0.275 wt.%. For synthetic purposes ash residue is not a critical parameter; however, from combustion perspectives it is an important property of the bio-oil (Zhang *et al.* 2007). The measured higher heating value of the bio-oil was 39.21 MJ/kg, which is comparable with the results

reported earlier in case of liquefaction oils (Itoh *et al.* 1994; Xiu *et al.* 2010; Vardon *et al.* 2012; Duan *et al.* 2013; Wang *et al.* 2013); however, it is quite a lot higher than the typical higher heating value of 16-19 MJ/kg in case of pyrolysis oils (Huber *et al.* 2006). The higher heating value of the bio-oil is close to heating value of 41 to 43 MJ/kg for conventional fossil oil (Bridgwater *et al.* 1999), indicating the high energy density of the crude bio-oil. The high heating value of the bio-oil may be attributed to low water content and high density of lignin based derivatives (White 1987). This high heating value is expected to adversely affect the thermal stability of the bio-oil based PF resins and the fabricated boards utilizing such resins as binders.

The measured values of pH, total acid number, and total phenol content of the bio-oil are presented in Table 2.

Table 2. pH, Total Acid number, and Total Phenol Content of the Bio-oil

Chemical properties	
pH	6.6 (± 0.04)
Total acid number (TAN) (mgKOH/g)	36.72 (± 0.35)
Total phenol content (mgGAE/g)	210 (± 2.86)
*Each value represents an average of three samples (± SEM)	

The measured pH value of the bio-oil was 6.6, which is comparable with the results reported earlier in case of liquefaction oils (He *et al.* 2001a); however, it was much higher than the typical pH value of 2.5 in case of pyrolysis oils (Huber *et al.* 2006). The measured TAN value of the bio-oil was 36.72, which is comparable with the results reported earlier for liquefaction oils; however, it was much lower than the typical TAN value of ~100 in case of pyrolysis oils (Oasmaa *et al.* 2010). The less acidic pH and lower TAN value indicates the low corrosive nature of bio-oil produced by the liquefaction process. The pH and TAN values also indicate the low potential storage problems for crude bio-oil.

The measured value of total phenol content of the bio-oil was 210 mgGAE/g, which is slightly higher than the reported total phenol content of ~190 mgGAE/g for liquefied alkaline lignin (Kang *et al.* 2010). It means that in terms of gallic acid the bio-oil contained 3.70×10^{-3} mol/g hydroxyl groups and 1.23×10^{-3} mol/g carboxylic groups. Thus the cumulative content of hydroxyl and carboxylic groups present in the bio-oil was roughly half of the hydroxyl group content of the pure phenol which is 1.063×10^{-2} mol/g. Hence, on rough basis the bio-oil is expected to show half of the reactivity of the pure phenol. The concentration of hydroxyl groups (3.70×10^{-3} mol/g) present in the bio-oil calculated in terms of gallic acid was higher than the reported concentration of phenolic hydroxyl groups (0.73×10^{-3}-1.47×10^{-3} mol/g) present in kraft lignin (Gellerstedt and Lindfors 1984). Hence in terms of total phenol content the crude bio-oil is generally expected to show higher reactivity than the lignin, and consequently expected to exhibit higher phenol substitution potential as compared to lignin in synthesis of BPF resins.

The GPC analysis of the crude bio-oil showed that bio-oil had a number-average molecular weight (M_n) of 471 (Da) and a weight-average molecular weight (M_w) of 1042 (Da), indicating that incorporation of bio-oil would cause an increase of molecular weights of the synthesized BPF resins. The GC-MS data showed that major compounds present in the bio-oil were mainly lignin based products such as 2-methoxy-4-(1-propenyl)-phenol, 2-methoxy-4-(2-propenyl)-phenol, 2-methoxy-phenol, 2-methyl-phenol, 2-methoxy-4-vinyl-phenol, 2, 6-dimethoxy-phenol, 2-methoxy-4-methylphenol,

4-ethyl-2-methoxyphenol, and phenol. The phenolic compounds made up approximately 53% of the bio-oil composition, followed in abundance by aldehydes, carboxylic acids, and ketones. The presence of high proportion of lignin based phenolic compounds in the bio-oil may be attributed to high lignin content of drupe endocarp feedstock (Dardick *et al.* 2010; Mendua *et al.* 2011). The GC-MS results are consistent with the findings of other research reports regarding molecular composition of the liquefaction oils (Cheng *et al.* 2010; Tymchyshyn and Xu 2010; Li *et al.* 2013; Liu *et al.* 2014), and report regarding molecular composition of the drupe endocarps (Mendu *et al.* 2011). The high percentage of phenolic compounds in the bio-oil is expected to enhance its phenol replacement potential in synthesis of BPF resins.

Properties of the Synthesized Resins

The GPC profiles of all the resins are exhibited in Fig. 1, and the measured values of M_n, M_w, range M_w % (M_w distribution), and polydispersity of all the resins are presented in Table 3. The M_n values of all the resins ranged from 363 to 608 (Da), while the M_w values of all the resins ranged from 724 to 1621 (Da). The values of polydispersity of all the resins ranged from 1.99 to 2.67.

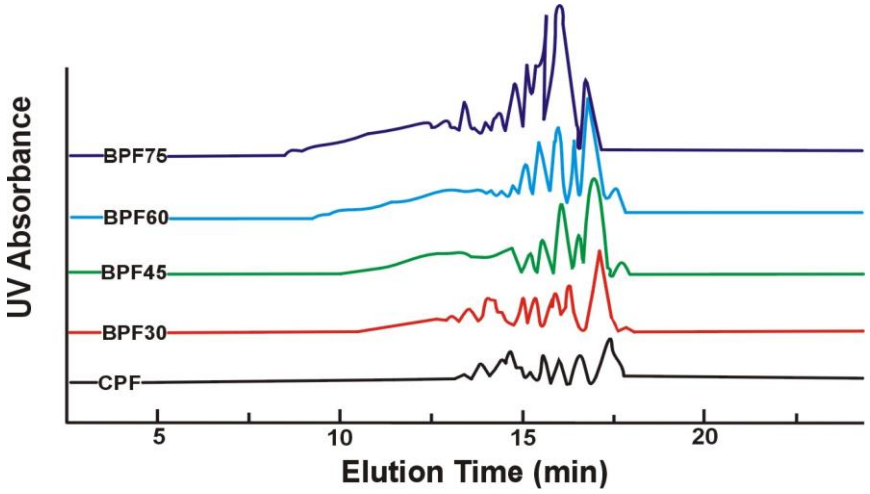

Fig. 1. GPC profiles of resins with different BOI%

Table 3. Number Average Molecular Weight (M_n), Weight Average Molecular Weight (M_w), Range M_w %, and Polydispersity of the Resins

Resin Code	BOI (%)	M_n Da	M_w Da	Range M_w %		Polydispersity (M_w/M_n)
				≤1000Da	>1000Da	
CPF	0	363 (± 1.78)	724 (± 1.31)	71 (0.90)	29 (0.90)	1.99
BPF30	30	482 (± 0.93)	1054 (± 2.18)	54 (0.36)	46(0.36)	2.19
BPF45	45	536 (± 1.26)	1291 (± 1.86)	47 (0.43)	53 (0.43)	2.41
BPF60	60	575 (± 2.05)	1489 (± 2.42)	43 (0.50)	57 (0.50)	2.59
BPF75	75	608 (± 1.93)	1621 (± 2.75)	41 (0.62)	59 (0.62)	2.67
*Each value represents an average of three samples (± SEM) BOI%: Bio-Oil Incorporation percentage in the resin formula						

GPC profiles of the resins exhibited in Fig. 1 demonstrate that with the increase of BOI level in the resin, the molecular weight distribution gradually widened and the peaks of distribution curves gradually shifted to higher molecular weight positions. The results displayed in Table 3 indicate that values of M_n, M_w, high M_w (>1000Da) resin fraction, and polydispersity gradually increased with the increase of BOI level, while the low M_w (≤1000Da) resin fraction gradually decreased with the increase of BOI level. The pattern of molecular weights exhibited by the BPF resins is more or less consistent with the reports of similar earlier studies (Wang *et al.* 2009a; Cheng *et al.* 2011). The gradual increase in M_n and M_w, and high M_w (>1000Da) resin fraction of the BPF resins may be attributed to incorporation of large and complex bio-oil molecules into the resin structure, as indicated by GPC and GC-MS studies of the bio-oil. The gradual increase in molecular weights of the BPF resins may also be attributed to catalytic effect of ligno-cellulosic derivatives present in bio-oil on the resin synthesis reaction, as indicated by an earlier study (Hu *et al.* 2013).

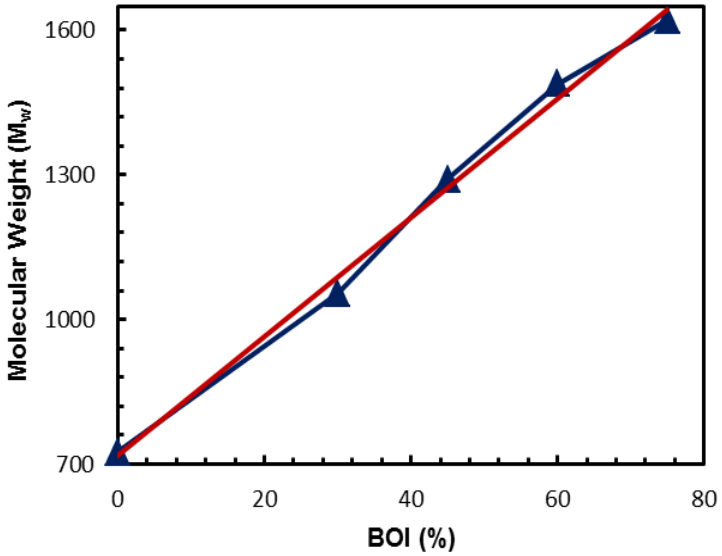

Fig. 2. Rate of change of weight average molecular weight (M_w) of resins with BOI%

Figure 2 shows the rate of change of weight average molecular weight (M_w) of the resins with the increase of BOI level. It is notable that in Fig. 2 mean values are used as a method to simplify the graphs, and plots of mean values are just for illustrative purpose. From graph plotted in Fig. 2, it appeared that molecular weight of the resins increased continuously with the increase of BOI level; however the rate of increase of molecular weight started relatively decreasing after the 45% BOI level, and this situation continued up to 75% BOI level. From 45 to 60% BOI level the decrease in increase rate of molecular weight was very slight but noticeable; however after 60% BOI level, the rate of increase of molecular weight started decreasing considerably. This relative decline in increase rate of molecular weights may be attributed to relatively less reactivity of the bio-oil, as indicated indirectly by its measured total phenol content listed in Table 2, as reported in literature (Lee *et al.* 2000; Wen *et al.* 2013). It may be presumed that beyond 45% BOI level, when bio-oil becomes the major substrate available for reaction with formaldehyde during the methylolation stage of resin synthesis reaction, the chemistry of resulting methylols is primarily determined by the amount of bio-oil. Because of a shortage of accessible active sites on the bio-oil molecules (Lee *et al.* 2000), as indicated

indirectly by its measured total phenol content, the rate of the methylolation reaction of the bio-oil would be relatively less as compared to rate of the methylolation reaction of the petro-phenol. It is again expected that bio-oil-based-methylols would have fewer polymerization points as compared to petro-phenol-based-methylols, thus implying that the extent of crosslinking of these bio-oil-based-methylols would be relatively lesser during the condensation stage of the synthesis reaction. Due to relatively less reactivity of the bio-oil (Lee *et al.* 2000; Wen *et al.* 2013), the extent of the condensation reaction is expected to be less during the resin synthesis reaction, as reported in the literature (Effendi *et al*. 2008). Generally, the extent of resin condensation reaction is directly related with the increase in molecular weights of the resins; hence beyond 45% BOI level, the increase in molecular weights slows down. The decline of increase in resin molecular weights may also be attributed to decreasing pH level of the reaction medium, as it is generally believed that extent of condensation reaction is directly related to the pH of the reaction medium.

Physical Properties of the Synthesized Resins

The measured values of pH, density, and viscosity of all the resins are presented in Table 4. The pH values ranged from 12.41 to 12.91, while the density ranged from 1.175 to 1.181 (g/cm^3). The viscosity of all the resins ranged from 302 to 411 (cP).

Table 4. The pH, Density, and Viscosity (at 25 °C) of the Resins

Resin code	BOI (%)	pH	Density (g/cm^3)	Viscosity (cP)
CPF	0	12.91 (± 0.031)	1.181 (± 0.015)	302 (± 1.7)
BPF30	30	12.74 (± 0.016)	1.180 (± 0.022)	357 (± 2.1)
BPF45	45	12.65 (± 0.023)	1.178 (± 0.019)	386 (± 1.3)
BPF60	60	12.54 (± 0.031)	1.176 (± 0.021)	399 (± 1.6)
BPF75	75	12.41 (± 0.025)	1.175 (± 0.017)	411 (± 1.4)
*Each value represents an average of three samples (± SEM) BOI%: Bio-Oil Incorporation percentage in the resin formula				

The results displayed in Table 4 show the effect of bio-oil incorporation on physical properties of the synthesized resins. In general, the values of pH and density of the resins gradually decreased with the increase of BOI level, while the viscosity gradually increased as the BOI level was increased. The gradual decrease of pH may be attributed to neutralization of the added alkali content (NaOH) by the acidic crude bio-oil (pH 6.6) due to presence of organic acids present, as reported in the literature (Sukhbaatar *et al.* 2009; Oasmaa *et al.* 2010; Hu *et al*. 2013). The decrease in density may be attributed to the increase in hydrodynamic volume of the BPF resins due to the incorporation of large bio-oil molecules. Due to high molecular weights and steric effect of bulky functional groups, the bio-oil molecules occupy large hydrodynamic volumes; thus, incorporation of such large bio-oil molecules decreases the mass to volume ratio (density) of the resulting resins. The gradual increase in viscosity may be attributed to increase in molecular weights of the BPF resins as indicated by Table 3. The increase in viscosity may also be attributed to increased entanglements of the BPF resin chains due to bulky functional groups attached on bio-oil molecules. The increased mutual entanglement of the resin chains may cause hindrance to the flow of the resulting resin solutions, thus increasing the viscosity.

The viscosity of a resin is an important physical property that affects its movement and flow behavior. Highly viscous resins are more resistant to deformation by stress and flow less easily, while the less viscous resins flow more easily and are less stress-resistant during different physical applications. The kinematic viscosity is another interesting parameter which may be calculated from Table 4 for analyzing the experimental data to check the suitable BOI level in the PF resin formulation. Kinematic viscosity, by contrast, measures the resistance of the resin to move or flow in the presence of gravity. This measure may be obtained by taking the resins' viscosity and dividing it by the resins' density. The higher the viscosity of the resins, the less easily it would move under the force of gravity and the higher its kinematic viscosity would be.

After converting the units of viscosity (cP) in gm/cm-sec, the results of the replicates were graphed against the BOI%, as shown in Fig. 3a.

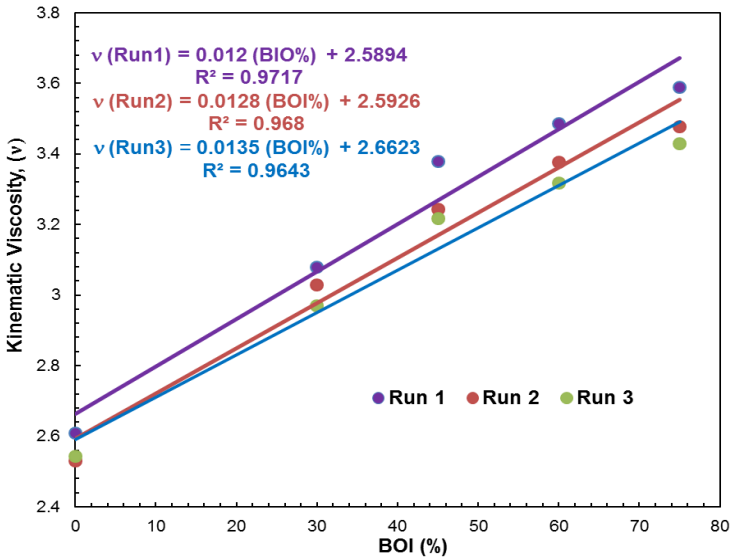

Fig. 3a. Replicates of kinematic viscosity of resins with different BOI%

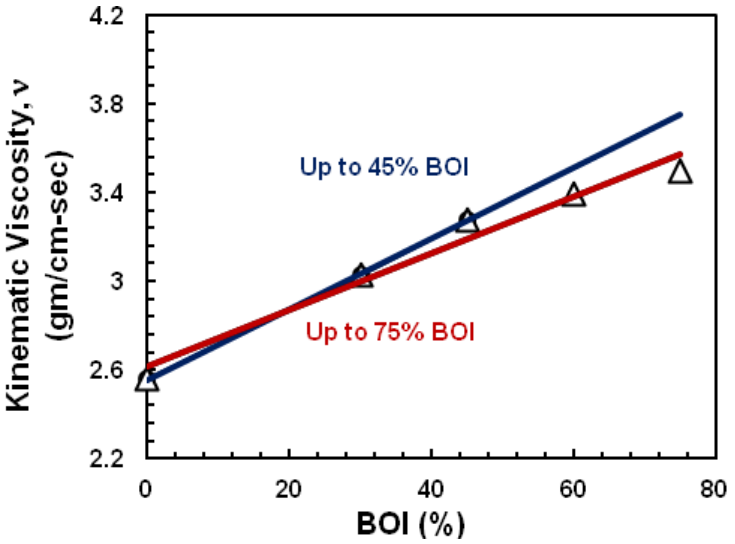

Fig. 3b. Kinematic viscosity of resins with different BOI%

As shown in Fig. 3a, the values of coefficient of determination (R^2) were almost equally good for all the three replicates. The graph shows that the kinematic viscosity of the resins was a linear function of BOI level in the resin. It is worth mentioning that mean values can be used as a method to simplify the graphs and plots just for illustrative purposes. Using the mean values of kinematic viscosity against the BOI level, the results have also been shown in Fig. 3b. The graphical results showed that up to 75% BOI level, the relationship between the variables was not very good. On the other hand, up to 45% BOI level, the correlation between the variables was found to be excellent with the coefficient of determination (R^2) 0.9997.

When the variables strongly correlate with each other, a semi-empirical model may be developed by graphical and statistical regression analysis (Zafar 2008; Zafar and Ashraf 2007; Zafar *et al*. 2008). The results in Fig. 3b show that the kinematic viscosity of the resins is a strong linear function of BOI level up to 45%, following a semi-empirical model,

$$\upsilon = Z_{IZ} + S_{AS}(BOI) \quad (1)$$

where ν is kinematic viscosity, Z_{IZ} is a constant factor, and S_{AS} is the sensitivity coefficient of the resins. Kinematics viscosity data was analyzed by graphical and statistical regression to determine the values of these constants, Z_{IZ}=2.5547 and S_{AS}=0.0159. Thus Eq. 1 is given as:

$$\upsilon = 2.5547 + 0.0159(BOI) \quad (2)$$

The constant (S_{AS}=0.0159) is the value of kinematics viscosity per unit value of incorporated bio-oil. The constant (Z_{IZ}=2.5547) is the value of kinematic viscosity without incorporation of bio-oil (BOI=0). This predicted value (Z_{IZ}=2.5547) by the suggested model is excellently comparable with the experimental value of kinematic viscosity, which is 2.5571 along with the residual value of 0.0024. On the other hand, the values of correlation coefficient (r=0.9997), coefficient of determination (R^2=0.9998), and standard error of estimates (SE=0.00914) indicate that the applicability of the model is very good supporting the incorporated level of bio-oil up to 45%.

Thermal Properties of the Synthesized Resins

The measured mean values of the gel and cure time of all the resins are portrayed in Fig. 4. The gel time of all the resins ranged from 5.94 to 10.09 (minutes), while the cure time of all the resins ranged from 3.20 to 6.40 (minutes). It is worth mentioning that mean values are used as a method to simplify the graphs and plots just for illustrative purpose.

Figure 4 indicates that both gel and cure time of the resins initially decreased with the incorporation of bio-oil; however the gel/cure times started increasing when BOI level exceeded the limit of *ca*. 45%. It was found that the gelation and curing pattern of the BPF45 resin was quite similar to the gelation and curing pattern of the CPF resin.

The initial decrease in gel/cure time may be attributed to increase in molecular weights of the resin, as it is generally believed that lower activation energy is needed for high molecular weight resins to gel/cure (Anwar *et al*. 2009; Wahab *et al*. 2012). The decrease in gel/cure time may also be attributed to catalytic effect of ligno-cellulosic derivatives present in crude bio-oil, as reported earlier by similar studies (Lei and Wu 2006; Wang *et al*. 2009b). The role of bio-oil as an efficient cross-linking agent due to

presence of multiple reactive sites (Hu *et al*. 2013) may also be taken as a reason for such decrease in gel/cure times. It is worth nothing that extent of decrease in gel time was relatively higher as compared to decrese in cure time, which may afford the molten resin a greater time lag for spreading and penetration during various applications.

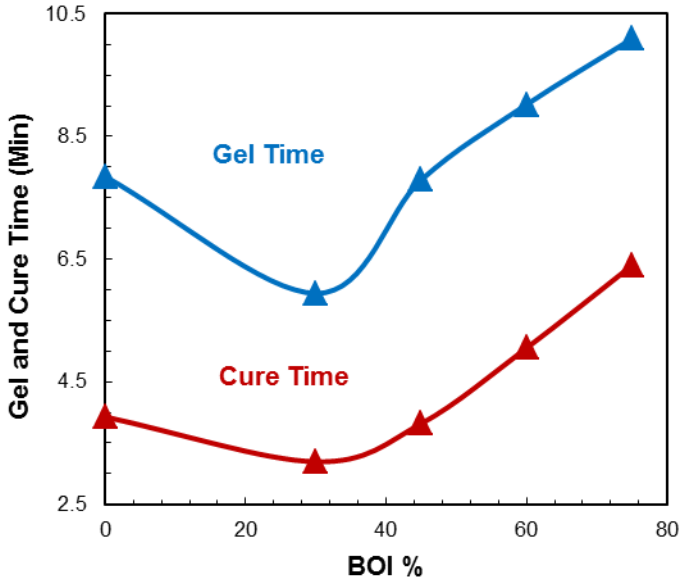

Fig. 4. Gel and cure time (mean value) of resins with different BOI%

The increase in gel/cure times of the BPF resins when the BOI level exceeded the limit of 45% is against the general principal of decreasing gel/cure times with increasing molecular weight of the resin. The increase in gel/cure time, which implies low polymerization reactivity of the resin, may be explained as an effect of the relatively lower reactivity indicated by its measured total phenol content, as cited in literature (Lee *et al*. 2000). It is assumed that the factor of less reactivity of the bio-oil translated itself into production of BPF resins having lower density of potential polymerization points required for cross-linking at gelation/curing stages. Beyond 45% incorporation levels, when bio-oil became the major substance in the synthesis reaction, the decline in density of polymerization points became significant enough, and thus gel/cure times started increasing due to decreased polymerization reactivity of the synthesized BPF resins.

The gel/cure test results expressed by Fig. 4 suggest that, depending on the incorporation level, the bio-oil can play two opposite and effective roles in the process of gelation/curing. At low incorporation level (< 45%) the bio-oil would favor the gelation and curing reactions, while at high incorporation level (> 45%) the bio-oil would exert a retarding effect on gelation/curing reactions.

The measured values of non-volatile solid content and LOI for all the resins are presented in Table 5. The values of non-volatile solid content ranged from 42.85% to 46.72%, while the values of LOI ranged from 25.9 to 35.5. Data in the table show the effects of bio-oil incorporation on non-volatile solid content and LOI values, indicating that both of the parameters gradually decreased with the increase of BOI level. The decrease in nonvolatile solid content may be attributed to relatively unstable structures of the bio-oil molecules, as explained in preceding paragraphs in bio-oil section. The incorporation of such unstable molecules renders the BPF resins thermally unstable, resulting in low yield of non-volatile solid content when heated for quantification study.

Table 5. Non-volatile Solid Content and Limiting Oxygen Index Values of the Resins

Resin Code	BOI (%)	Non-volatile solid content (%)	LOI
CPF	0	46.72 (± 0.21)	35.5 (± 0.23)
BPF30	30	45.23 (± 0.18)	32.1 (± 0.34)
BPF45	45	44.32 (± 0.27)	30.4 (± 0.21)
BPF60	60	43.02 (± 0.20)	28.7 (± 0.30)
BPF75	75	42.85 (± 0.13)	25.9 (± 0.19)
*Each value represents an average of three samples (± SEM) BOI%: Bio-Oil Incorporation percentage in the resin formula; LOI: Limiting Oxygen Index			

The weight loss during thermal heating may also be attributed to thermal degradation of cellulosic impurities, and removal of water and other volatile molecules present in the crude bio-oil. The structural instability of bio-oil molecules may be attributed to the presence of unsaturated double bonds, oxygenated molecules (He *et al.* 2001b; Yao *et al*. 2008), and side chains attached on bio-oil molecules (Wang *et al.* 2009a). During heating for quantification of non-volatile solid content a number of reorganization and repolymerization reactions are involved, as reported in literature (Khan and Ashraf 2007; Chen *et al.* 2008; Wang *et al.* 2009a; Cheng *et al.* 2011, 2012).

The decrease of LOI values may be attributed to high energy value of the bio-oil, as indicated by its higher heating value enlisted in Table 1, as cited in literature (Czernik and Bridgwater 2004; Zhang *et al.* 2007; Lu *et al*. 2009; Venderbosch and Prins 2010). The decrease in values of non-volatile solid content and the limiting oxygen index of the BPF resins amounts to decrease in their thermal stability. This decrease in thermal stability due to incorporation of bio-oil is still a challenging issue faced during synthesis of such resins.

Bonding Properties of the Synthesized Resins

Operational/manufacturing properties of the synthesized resins

All the synthesized resins showed normal behavior during the development of particle boards. During spraying of resin solution on the wood particle mass, there was not much build-up of the resin in the sprayer or inside the blender drum, indicating that application of BPF resins would not create any operational problems. Similarly, all the resin samples behaved well during various stages of board fabrication like formation of loose mat, cold pressing, and the hot pressing stages.

Mechanical properties of the developed particle boards

Table 6 displays the MOR and IB values of the developed particle board samples. The MOR values of all the board samples ranged from 24.4 to 42.7 MPa while the IB values ranged from 481 to 993 KPa.

Table 6, which exhibits the mechanical strength of the board samples, indicates that the MOR/IB values initially increased with the incorporation of bio-oil; however, these started decreasing after 45% BOI level. The MOR/IB results of various samples indicate that B.BPF45 board sample utilizing the BPF45 (BOI=45%) resin as binder demonstrated mechanical performance comparable to mechanical performance of B.CPF board sample utilizing CPF (BOI=0%) resin.

Table 6. Modulus of Rupture (MOR) and Internal Bond Strength (IB) of the Board Samples

Board Code	BOI (%)	MOR (MPa)	IB (KPa)
B.CPF	0	38.5 (± 0.33)	879 (± 1.14)
B.BPF30	30	42.7 (± 0.31)	993 (± 2.09)
B.BPF45	45	39.1 (± 0.37)	881 (± 1.78)
B.BPF60	60	31.9 (± 0.25)	697 (± 1.56)
B.BPF75	75	24.4 (± 0.43)	481 (± 2.31)
*Each value represents an average of three samples (± SEM) BOI%: Bio-Oil Incorporation percentage in the resin formula			

The penetration capacity of binder resins is inversely proportional to their molecular weights (Johnson and Kamke 1992; Johnson and Kamke 1994), and generally the resins with M_w>1000Da cannot penetrate effectively into nano-sized cell wall pores (Stamm 1964; Robison 1972; Sellers 1994), and thus remain limited to micro/macro sized pores/cavities of wood matrix. During hot press application, the resin present in pores/cavities of all sizes (nano/micro/macro) cures (Laborie 2002; Huang *et al.* 2012) into a solid interpenetrating polymer network, which interlocks the matrix material mechanically (Browne and Brouse 1929). In addition to providing mechanical strength to cell walls (Furuno *et al.* 2004; Huang *et al.* 2012), the resin fraction penetrating into cell walls is also presumed to provide anchoring points to the entire polymer network.

From reports cited in literature (Stamm 1964; Robison 1972; Sellers 1994), it can be inferred that, during hot pressing, the low M_w (≤1000Da) resin fraction penetrated into nano sized cell walls, while the high M_w (>1000Da) resin fraction remained limited to micro/macro sized pores/cavities. With the gradual increase in resin molecular weight the nano-scale resin penetration decreased gradually. However, for an effective bonding an optimal resin penetration into pores of all sizes (nano/micro/macro) and optimal curing is required, which is only possible when a resin having suitable combination of gel/cure times and molecular weight distribution, in reference to pores chemistry of subject wood matrix, is applied as binder. From the data of gel/cure times displayed in Fig. 4, molecular weight distribution given in Table 3, and MOR/IB values exhibited in Table 6, it can be assumed that BPF45 resin attained that suitable combination of gel/cure times and molecular weight distribution, which resulted in optimal penetration/curing, and consequently established the solid polymer network interlocking the wood matrix with optimal mechanical strength.

The initial increase in MOR/IB values of the board samples may be attributed to increase in the high M_w (>1000Da) resin fraction, as indicated by Dunky (1997), and to decrease in gel/cure time of the resins. However beyond 45% BOI level, based on decreasing low $\underline{M}_w$ (≤1000Da) resin fraction and MOR/IB values, and increasing gel/cure times, it is presumed that resin fraction penetrating into cell wall pores decreased significantly, and thus the mechanical strength of cell walls started decreasing, as indicated in literature (Furuno *et al.* 2004; Huang *et al.* 2012). It is further assumed that beyond 45% BOI, due to increased gel/cure times, cured polymer network having lower mechanical interlocking strength was formed. Thus the decrease in mechanical/bonding strength of board samples, after 45%BOI level, may be attributed to cumulative effect of decrease in low M_w (<1000Da) resin fraction, and to increase in gel/cure times of the BPF resins.

Hygroscopic properties of the developed particle boards

The measured values of boiled internal bond residual strength (IB-RS), thickness swelling (TS), and water absorption (WA) of the board samples are presented in Table 7. The values of IB-RS of all the board samples ranged from 29% to 51%, while the TS values ranged from 16.9% to 35.2%. The WA values of all the board samples ranged from 22.9% to 49.2%.

Table 7. Internal Bond Residual Strength (IB-RS %), Thickness Swelling (TS %), and Water Absorption (WA %) of the Board Samples

Board Code	BOI (%)	IB-RS (%)	2 h Water Boiling	
			TS (%)	WA (%)
B.CPF	0	43 (± 0.39)	19.1 (± 0.13)	25.6 (± 0.21)
B.BPF30	30	51 (± 0.41)	16.9 (± 0.17)	22.9 (± 0.17)
B.BPF45	45	45 (± 0.32)	18.9 (± 0.21)	25.1 (± 0.18)
B.BPF60	60	38 (± 0.35)	24.9 (± 0.18)	32.9 (± 0.25)
B.BPF75	75	29 (± 0.43)	35.2 (± 0.25)	49.2 (± 0.23)
*Each value represents an average of three samples (± SEM) BOI%: Bio-Oil Incorporation percentage in the resin formula				

Table 7 indicates that TS/WA values initially decreased with the incorporation of bio-oil; however these started increasing when BOI level exceeded the limit of 45%. Similarly, the IB-RS value initially increased with the incorporation of bio-oil; however, it started decreasing when BOI level exceeded the limit of 45%. The results displayed in Table 7 demonstrate that initially the hygroscopic strength of the board samples increased with the incorporation of bio-oil; however, it started decreasing when BOI level exceeded the limit of 45%. The results indicate that B.BPF45 board sample utilizing BPF45 (BOI=45%) resin as binder demonstrated hygroscopic strength comparable to hygroscopic strength of B.CPF board sample utilizing CPF (BOI=0%) resin.

In addition to providing mechanical strength to the matrix cell walls (Furuno *et al.* 2004; Huang *et al.* 2012), the resin fraction penetrating into cell walls also establishes intermolecular couplings with ligno-cellulosic matrix and blocks the hydrophilic (-OH) moieties present on cellulose fibers (Huang *et al.* 2012). Due to blockage of hydrophilic (-OH) moieties the lesser amount of water is absorbed by the cell walls, and consequently less rupturing stress is exerted on the interlocking polymer network.

The initial increase in hygroscopic strength of the boards may be attributed to increased mechanical strength of the boards expressed in terms of increased MOR/IB, as shown in Table 6, and to chemical bonding effect of the resin fraction penetrating into the cell walls (Huang *et al.* 2012). The increased hygroscopic stability of the board samples may also be attributed to hydrophobic character of the crude bio-oil incorporated in the BPF resins (Robinson *et al.* 2011).

The decrease in hygroscopic strength of the board samples may be attributed to decrease in low $\underline{M}_w$ (<1000Da) resin fraction as shown in Table 3, decrease in MOR/IB value as given in Table 6, and to increase in resin gel/cure times as indicated by Fig. 4. It is presumed that beyond 45% BOI level the nano scale resin penetration required for chemical bonding fell below the optimal level, and thus the dimensional stability of the wood started decreasing, probably due to increased water uptake by the hydrophilic cell walls. Due to increased dimensional changes of wood matrix, more rupturing stress was exerted on the interlocking polymer network. Thus, beyond 45% BOI level, the decrease

in hygroscopic strength of the boards samples may be attributed to increased rupturing stress, and to decreased mechanical interlocking strength.

It is pertinent to mention that regarding some other aspects, the BPF resins need further investigation, which is expected to be presented in the next research work. The design parameters may demand further studies at an industrial level; however, the present work may be of some value to others confronted with the need to use such typical bio-oil waste materials in various countries of the world.

CONCLUSIONS

1. Crude bio-oil was prepared from drupe endocarp shells of *Ziziphus mauritiana* by direct solvolytic liquefaction method (ethanol-water 1:1 wt./wt. at 300 °C).
2. The crude bio-oil was used to substitute petro-phenol up to 75% in the synthesis of bio-oil based phenol formaldehyde (BPF) resol resins.
3. The experimental results of various analytical and statistical tests revealed that, up to 45% BOI level, the BPF resins exhibited acceptable levels of viscosity, gel/cure times, thermal stability, and bonding performance.
4. Higher level of bio-oil incorporation (> 45% wt./wt.) in the synthesis process compromised various physical, thermal, and bonding properties of the BPF resins considerably.

REFERENCES CITED

ASTM-D240-09. (2009). "Standard test method for heat of combustion of liquid hydrocarbon fuels by bomb calorimeter," *ASTM International*, West Conshohocken, PA.

ASTM D482-13. (2013). "Standard test method for ash from petroleum products," *ASTM International*, West Conshohocken, PA.

ASTM D664-11. (2011). "Standard test method for acid number of petroleum products by potentiometric titration," *ASTM International*, West Conshohocken, PA.

ASTM-D1037-99. (1999). "Standard test methods for evaluating properties of wood base fibre and particle panel materials," *ASTM International*, West Conshohocken, PA.

ASTM-D1084-97. (2005). "Standard test methods for viscosity of adhesives," *ASTM International*, West Conshohocken, PA.

ASTM D1744-13. (2013). "Standard test method for determination of water in liquid petroleum products by Karl Fischer reagent," *ASTM International*, West Conshohocken, PA.

ASTM-D2863-77. (1990). "Standard test methods for measuring the minimum oxygen concentration to support candle-like combustion of plastics (oxygen index)," *ASTM International*, West Conshohocken, PA.

ASTM-D4426-01. (2006). "Standard test methods for determination of percent nonvolatile content of liquid phenolic resins used for wood laminating," *ASTM International*, West Conshohocken, PA.

ASTM D4530-11. (2011). "Standard test method for determination of carbon residue-Micro method," *ASTM International*, West Conshohocken, PA.

ASTM D5018-89. (2009) "Standard test method for shear viscosity of coal-tar and petroleum pitches," *ASTM International*, West Conshohocken, PA.

Alma, M. H., Basturk, M. A., and Shiraishi, N. (2001). "Co-condensation of NaOH-catalyzed liquefied wood wastes, phenol, and formaldehyde for production of resol-type adhesives," *Ind. Eng. Chem. Res.* 40(22), 5036-5039.

Alma, M. H., and Basturk, M. A. (2006). "Liquefaction of grapevine cane (*Vitis vinisera* L.) waste and its application to phenol-formaldehyde type adhesive," *Ind. Crops Prod.* 24(2), 171-176.

Amen-Chen, C., Riedl, B., and Roy, C. (2002). "Softwood bark pyrolysis oil-PF resols. Part 2.Thermal analysis by DSC and TG," *Holzforschung* 56(3), 273-280.

Anwar, U. M. K., Paridah, M. T., Hamdan, H., Sapuan, S. M., and Bakar, E. S. (2009). "Effect of curing time on physical and mechanical properties of phenolic-treated bamboo strips," *Ind. Crops Prod.* 29(1), 214-219.

Briens, C., Piskorz, J., and Berruti, F. (2008). "Biomass valorization for fuel and chemicals production - A review," *Int. J. Chem. React. Eng.* 6(1), R2.

Bridgwater, A. V., Czernik, S., Diebold, J., Meier, D., Oasmaa, A., Peacocke, C., Piskorz, J. and Radlein, D. (1999). *Fast Pyrolysis of Biomass: A Handbook*, CPL Scientific publishing services limited, Newbury, UK.

Browne, F. L., and Brouse, D. (1929). "Nature of adhesion between glue and wood. 1: A criticism of the hypothesis that the strength of glued wood joints is due chiefly to mechanical adhesion," *Ind. Eng. Chem.* 21(1), 80-84.

Chen, Y., Chen, Z., Xiao, S., and Liu. H. (2008). "A novel thermal degradation mechanism of phenol-formaldehyde type resins," *Thermochimica Acta* 476(1), 39-43.

Cheng, S., D'Cruz, I., Wang, M., Leitch, M., and Xu, C. (2010). "Highly efficient liquefaction of woody biomass in hot-compressed alcohol-water co-solvent," *Energ. Fuel* 24(9), 4659-4667.

Cheng, S., D'Cruz, I., Yuan, Z., Wang, M., Anderson, M., Leitch, M., and Xu, C. C. (2011). "Use of biocrude derived from woody biomass to substitute phenol at a high-substitution level for the production of biobased phenolic resol resins," *J. Appl. Polym. Sci.* 121(5), 2743-2751.

Cheng, S., D'Cruz, I., Yuan, Z., Wang, M., Anderson, M., Leitch, M., and Xu, C. C. (2012). "Synthesis of bio-based phenolic resins/adhesives with methylolated wood derived bio-oil," *J. Appl. Polym. Sci.*126 (S1), E430-E440.

Czernik, S., and Bridgwater, A. V. (2004). "Overview of applications of biomass fast pyrolysis oil," *Energ. Fuel* 18(2), 590-598.

Dardick, C., Callahan, A., Chiozzotto, R., Schaffer, R., Piagnani, M. C., and Scorza, R. (2010). "Stone formation in peach fruit exhibits spatial coordination of the lignin and flavonoid pathways and similarity to *Arabidopsis dehiscence*," *BMC Biol.* 8, 13.

Diebold, J. P. (2000). "A review of the chemical and physical mechanisms of the storage stability of fast pyrolysis bio-oils," NREL/SR-570-27613, Golden, Colorado

Duan, P., Chang, Z., Xu, Y., Bai, X., Wang, F., and Zhang, L. (2013). "Hydrothermal processing of duckweed: Effect of reaction conditions on product distribution and composition," *Bioresour. Technol.* 135(1), 710-719.

Dunky, M. (1997). "Analysis of formaldehyde condensation resins for the wood based panels industry: Status and new challenges," *Proceedings of the Seventh European Panels Products Symposium*, Llandudno, North Wales, UK.

Effendi, A., Gerhauser, H., and Bridgwater, A. V. (2008). "Production of renewable phenolic resins by thermochemical conversion of biomass: A review," *Renew. Sust. Energy Rev.* 12(8), 2092-2116.

Elliott, D. C., Beckman, D., Bridgwater, A. V., Diebold, J. P., Gevert, S. B., and Solantausta, Y. (1991). "Developments in direct thermochemical liquefaction of biomass: 1983-1990," *Energ. Fuel* 5(3), 399-410.

Elliott, D. C., and Schiefelbein, G. F. (1989). "Liquid hydrocarbon fuels from biomass," *Pap. Am. Chem. Soc.* 34(4), 1160-1166

Frihart, C. R. (2005). "Wood adhesion and adhesives," in: *Handbook of Wood Chemistry and Wood Composites*, R. M. Rowell (ed.), CRC Press, Boca Raton, FL.

Furuno, T., Imamura, Y., and Kajita, H. (2004). "The modification of wood by treatment with low molecular weight phenol-formaldehyde resin: A properties enhancement with neutralized phenolic-resin and resin penetration into wood cell walls," *Wood Sci. Technol.* 37(5), 349-361.

Gani, A., and Naruse, I. (2007). "Effect of cellulose and lignin content on pyrolysis and combustion characteristics for several types of biomass," *Renew. Energ.* 32(4), 649-661.

Gellerstedt, G., and Lindfors, E. (1984). "Structural changes in lignin during kraft cooking. Part 4. Phenolic hydroxyl groups in wood and kraft pulps," *Svensk Papperstidn*. 87(15), R115-R118.

Gutfinger, T. (1981). "Polyphenols in olive oils," *J. Am. Oil Chem. Soc.* 58(11), 966-968.

He, B., Zhang, Y., Yin, Y., Funk, T. L., and Riskowski, G. L. (2001a). "Effects of feedstock pH, initial CO addition, and total solids content on the thermochemical conversion process of swine manure," *T. Am. Soc. Agr. Eng.* 44(3), 697-704.

He, B. J., Zhang, Y., Yin, Y., Funk, T. L., and Riskowski, G. L. (2001b). "Preliminary characterization of raw oil products from the thermochemical conversion of swine manure," *T. Am. Soc. Agr. Eng.* 44(6), 1865-1872.

Hu, X., Wang, Y., Mourant, D., Gunawan, R., Lievens, C., Chaiwat, W., Gholizadeh, M., Wu, L., Li, X., and Li, C. Z. (2013). "Polymerization on heating up of bio-oil: A model compound study," *AIChE J.* 59(3), 888-900.

Huang, Y., Fei, B., Yu, Y., and Zhao, R. (2012). "Effect of modification with phenol formaldehyde resin on the mechanical properties of wood from Chinese Fir," *BioResources* 8(1), 272-282.

Huber, G. W., Iborra, S., and Corma, A. (2006). "Synthesis of transportation fuels from biomass: chemistry, catalysts, and engineering," *Chem.Rev.* 106(9), 4044-4098.

Itoh, S., Suzuki, A., Nakamura, T., and Yokoyama, S. Y. (1994). "Production of heavy oil from sewage sludge by direct thermochemical liquefaction," *Desalination*, 98(1), 127-133.

Johnson, S. E., and Kamke, F. A. (1992). "Quantitative analysis of gross adhesive penetration in wood using fluorescence microscopy," *J. Adhesion*, 40(1), 47-61.

Johnson, S. E., and Kamke, F. A. (1994). "Characteristics of Phenol-Formaldehyde adhesive bonds in steam injection pressed flakeboard," *Wood Fiber Sci.* 26(2), 259-269.

Kang, S., Li, B., Chang, J., and Fan, J. (2010). "Antioxidant abilities comparison of lignins with their hydrothermal liquefaction products," *BioResources* 6(1), 243-252.

Khan, M. A., and Ashraf, S.M. (2007). "Studies on thermal Characterization of lignin substituted phenol formaldehyde resin as wood adhesives," *J. Therm. Anal. Calorim.* 89(3), 993-1000.

Knop, A., and Pilato, L. A. (1985). *Phenolic Resins, Chemistry Applications and Performance*, Springer-Verlag, New York.

Laborie, M. P. G. (2002). *Investigation of the Wood/Phenol-Formaldehyde Adhesive Interphase Morphology*, Ph. D. dissertation, Virginia Polytechnic Institute and State University, Blacksburg, VA.

Lee, S. H., and Ohkita, T. (2003). "Rapid wood liquefaction by supercritical phenol," *Wood Sci. Technol.* 37(1), 29-38.

Lee, S. H., Yoshioka, M., and Shiraishi, N. (2000). "Preparation and properties of phenolated corn bran (CB)-phenol formaldehyde co-condensed resin," *J. Appl. Polym. Sci.* 7(13), 2901-2907.

Lei, Y., and Wu, Q. (2006). "Cure kinetics of aqueous phenol-formaldehyde resins used for oriented strand board manufacturing: Effect of wood flour," *J. Appl. Polym. Sci.* 102(4), 3774-3781.

Li, C., Yang, X., Zhang, Z., Zhou, D., Zhang, L., Zhang, S., and Chen, J. (2013). "Hydrothermal liquefaction of desert shrub salix psammophila to high value-added chemicals and hydrochar with recycled processing water," *BioResources*, 8(2), 2981-2997.

Liu, H. M., Wang, F. Y., and Liu, Y. L. (2014). "Characterization of bio-oils from alkaline pretreatment and hydrothermal liquefaction (APHL) of Cypress," *BioResources* 9(2), 2772-2781.

Lu, Q., Li, W. Z., and Zhu, X. F. (2009). "Overview of fuel properties of biomass fast pyrolysis oils," *Energ. Convers. Manage.* 50(5), 1376-1383.

Mendu, V., Harman-Ware, A. E., Crocker, M., Jae, J., Stork, J., Morton, S., Placido, A., Huber, G., and DeBolt, S. (2011). "Identification and thermochemical analysis of high-lignin feedstocks for biofuel and biochemical production," *Biotechnol. Biofuel.* 4, 43.

Mendu, V., Shearin, T., Campbell, J. E., Stork, J., Jae, J., Crocker, M., Huber, G., and DeBolt, S. (2012). "Global bioenergy potential from high-lignin agricultural residue," *Proceedings of the NAS, USA* 109(10), 4014-4019.

Mun, S., Ku, C., and Park, S. (2007). "Physicochemical characterization of pyrolyzates produced from carbonization of lignocellulosic biomass in a batch-type mechanical kiln," *J. Ind. Eng. Chem.* 13(1), 127-132.

Oasmaa, A., and Kuoppala, E. (2003). "Fast pyrolysis of forestry residue. 3. Storage stability of liquid fuel," *Energ. Fuels* 17(1),1075-1084

Oasmaa, A. and Czernik, S. (1999). "Fuel oil quality of biomass pyrolysis oils state of the art for the end users," *Energ. Fuels* 13(4), 914-921.

Oasmaa, A., Elliott, D. C., and Korhonen, J. (2010). "Acidity of biomass fast pyrolysis bio-oils," *Energ. Fuel* 24(12), 6548-6554.

Özbay, N., Uzun, B. B., Varol, E. A., and Pütün, A. E. (2006). "Comparative analysis of pyrolysis oils and its subfractions under different atmospheric conditions," *Fuel Process. Technol.* 87(11), 1013-1019.

Robison, R.G. (1972). *Wood-Coating Interactions*, Ph. D. dissertation, State University College of Forestry at Syracuse University, Syracuse, NY.

Robinson, T. J., Via, B. K., Fasina, O., Adhikari, S., and Carter, E. (2011). "Impregnation of bio-oil from small diameter pine into wood for moisture resistance," *BioResources* 6(4), 4747-4761.

Sanchez, C. (2009). "Lignocellulosic residues: Biodegradation and bioconversion by fungi," *Biotechnol. Adv.* 27(2), 185-194.

Sellers Jr., T. (1985). *Plywood and Adhesive Technology*, Marcel Dekker, New York.

Sellers, Jr., T. (1994). "Adhesives in the wood industry," in: *Handbook of Adhesive Technology*, Pizzi, A., and Mittal, K. (eds.), Marcel Dekker, New York, New York, pp. 599-614.

Stamm, A. J. (1964). *Wood and Cellulose Science*, Ronald Press, New York, New York, pp. 312-342.

Sukhbaatar, B., Steele, P. H., Ingram, L. I., and Kim, M. G. (2009). "Use of lignin separated from bio-oil in oriented strand board binder phenol formaldehyde resins," *BioResources* 4(2), 789-804.

Tymchyshyn, M., and Xu, C. C. (2010). "Liquefaction of bio-mass in hot-compressed water for the production of phenolic compounds," *Biores. Technol.* 101(7), 2483-2490.

Vardon, D. R., Sharma, B. K., Blazina, G. V., Rajagopalan, K., and Strathmann, T. J. (2012). "Thermochemical conversion of raw and defatted algal biomass via hydrothermal liquefaction and slow pyrolysis," *Biores.Technol.*109(1), 178-187.

Venderbosch, R. H., and Prins, W. (2010). "Fast pyrolysis technology development," *Biofuels Bioprod. Bioref.* 4(2), 178-208.

Wahab, N. H. A., Tahir, P. M., Hoong, Y. B., Ashaari, Z., Yunus, N. Y. M., Uyup, M. K. A., and Shahri, M. H. (2012). "Adhesion characteristics of phenol formaldehyde pre-preg oil palm stem veneers," *BioResources* 7(4), 4545-4562.

Wang, F., Chang, Z., Duan, P., Yan, W., Xu, Y., Zhang, L., Miao, J., and Fan, Y. (2013). "Hydrothermal liquefaction of *Litsea cubeba* seed to produce bio-oils," *Biores.Technol.* 149(1), 509-515.

Wang, M., Leitch, M., and Xu, C. (2009a). "Synthesis of phenolic resol resins using cornstalk derived bio-oil produced by direct liquefaction in hot compressed phenol-water," *J. Ind. Eng. Chem.*15(6), 870-875.

Wang, M., Xu, C., and Leitch, M. (2009b). "Liquefaction of cornstalk in hot-compressed phenol-water medium to phenolic feedstock for the synthesis of phenol-formaldehyde resin," *Biores. Technol.* 100(7), 2305-2307.

Wen, M. Y., Shi, J. Y., and Park, H. J. (2013). "Dynamic wettability and curing characteristics of liquefied bark-modified phenol formaldehyde resin (BPF) on rice straw surfaces," *J. Wood Sc.* 59(3), 262-268.

Weng, J. K., Li, X., Bonawitz, N. D., and Chapple, C. (2008). "Emerging strategies of lignin engineering and degradation for cellulosic biofuel production," *Curr. Opin. Biotech.*19(2), 166-172.

White, R. H. (1987). "Effect of lignin content and extractives on the higher heating value of wood," *Wood fiber Sci.* 19(4), 446-452.

Xiu, S. N., Shahbazi, A., Croonenberghs, J., and Wang, L. J. (2010). "Oil production from duckweed by thermochemical liquefaction," *Energ. Sources, Part A*, 32(14), 1293-1300.

Xu, Y., Hanna, M. A., and Isom, L. (2008). "Green chemicals from renewable agricultural biomass – A mini review," *Open Agr. J.* 2(1), 54-61.

Yao, Y., Wang, S.R. and Luo, Z.Y. (2008). "Experimental research on catalytic hydrogenation of light fraction of bio-oil," *J. Eng. Thermophys.* 29(4), 715-719.

Zafar, Z. I., and Ashraf, M. (2007). "Selective leaching kinetics of calcareous phosphate rock in lactic acid," *Chem. Eng. J.* 131(1), 41-48.

Zafar, Z. I. (2008). "Determination of semi empirical kinetic model for dissolution of bauxite ore with sulfuric acid: Parametric cumulative effect on the Arrhenius parameters," *Chem. Eng. J.* 141(1-3), 233-241.

Zafar, Z. I., Malana, M. A., Pervez, H., Shad, M. A., and Momma, K. (2008). "Synthesis and swelling kinetics of a cross-linked pH-sensitive ternary co-polymer gel system," *Polymer (Korea)* 32(3), 219-229.

Zhang, Q., Zhao, G., and Chen, J. (2006). "Effects of inorganic acid catalysts on liquefaction of wood in phenol," *Front. For. China* 1(2), 214-218.

Zhang, Q., Chang, J., Wang, T., and Xu, Y. (2007). "Review of biomass pyrolysis oil properties and upgrading research," *Energ. Convers. Manage.* 48(1), 87-92.

Zhang, W., Ma, Y., Xu, Y., Wang, C., and Chu, F. (2013). "Lignocellulosic ethanol residue-based lignin-phenol-formaldehyde resin adhesive," *Int. J. Adhes. Adhes.* 40(1), 11-18.

Article submitted: March 31, 2014; Peer review completed: June 1, 2014; Revised version received and accepted: July 14, 2014; Published: July 21, 2014.